

A simplified method for calculating the ac Stark shift of hyperfine levels

Xia Xu,¹ Bo Qing,² Xuzong Chen,¹ and Xiaoji Zhou^{1,*}

¹*School of Electronics Engineering & Computer Science, Peking University, Beijing 100871, China*

²*Department of Physics, Tsinghua University, Beijing 100084, China*

The ac Stark shift of hyperfine levels of neutral atoms can be calculated using the third order perturbation theory (TOPT), where the third order corrections are quadratic in the atom-photon interaction and linear in the hyperfine interaction. In this paper, we use Green's function to derive the $E^{[2+\epsilon]}$ method which can give close values to those of TOPT for the differential light shift between two hyperfine levels. It comes with a simple form and easy incorporation of theoretical and experimental atomic structure data. Furthermore, we analyze the order of approximation and give the condition under which $E^{[2+\epsilon]}$ method is valid.

PACS numbers: 0.6.20-f; 0.6.30-Ft; 32.80.Qk; 32.30.Bv.

I. INTRODUCTION

The recent developments in precision measurement [1, 2] and optical communication [3] require a possible way to calculate the ac Stark shift with considerable precision. In many cases, the second order perturbation theory (SOPT) [4], which is capable of utilizing the existing theoretical and experimental atomic structure data, is used to compute the light shifts. For instance, in today's researches on atomic clocks, it has been realized that the accuracy and stability can be substantially improved by trapping cold atoms in a standing wave of light (optical lattice) [5–8]. Because of the minimization of Doppler and recoil effects, light shift caused by trapping laser is essential. Therefore the wavelength of the trapping laser should be tuned to a region where the light shifts of the two clock transition states cancel each other out. This wavelength is called “magic wavelength” [9]. In optical clocks and terahertz clocks, the clock transition is between the fine structure of atomic ground state and excited states, and we can utilize the SOPT to compute the light shift of the clock transition. The shift arises in the second order of perturbation theory which is quadratic in the electric field strength. The calculations suggest the existence of magic wavelength both for optical-clock transitions [10–13] and terahertz-clock transitions [14].

Recently, the alkali-metal atom like rubidium (Rb) and cesium (Cs) are considered as potential choices for microwave lattice clocks, using the two field insensitive hyperfine levels of the ground state as clock transition levels [15]. However, because SOPT doesn't take into account the hyperfine interaction, the results are identical for the hyperfine doublet of the ground state at arbitrary values of trapping laser wavelength. To solve this problem, the third order perturbation theory (TOPT) [20] was proposed by extending the formalism to the higher order of perturbation theory, and the third order corrections are quadratic in the field amplitude and linear in the hyperfine interaction. The theory requires using *ab initio* approach to construct the atomic structure database. Here we introduce the $E^{[2+\epsilon]}$ method which takes the hyperfine interac-

tions into consideration in SOPT. We will show that for a wide range of trapping laser wavelength, $E^{[2+\epsilon]}$ method gives close results to those of TOPT and experiments. In addition, $E^{[2+\epsilon]}$ method comes with a simple form, easy incorporation of theoretical and experimental atomic structure data, and therefore is more applicable for other group elements.

The remainder of this manuscript is organized as follows. We use Green's function and diagrammatic representation to derive the $E^{[2+\epsilon]}$ method in Sec.II. In Sec.III, the differential light shifts between two field insensitive hyperfine levels of the ground state of Cs and Rb are calculated using both methods, due to their potential application in microwave lattice clocks. In the calculation, besides utilizing the existing experimental atomic structure data, we use GraspVU code [16] to construct our own database of atomic structure, which is summarized in Appendix A. The discussions and conclusions are given in Sec.IV.

II. $E^{[2+\epsilon]}$ METHOD

A. Hyperfine structure

We start with no light fields. The Hamiltonian \hat{h} of the system can be written as the sum of the unperturbed part \hat{h}_0 and the perturbation $\Delta\hat{h}$.

$$\begin{aligned}\hat{h} &= \hat{h}_0 + \Delta\hat{h}, \\ \hat{h}_0 &= \hat{H}_{fs}, \\ \Delta\hat{h} &= \hat{H}_{hfs}.\end{aligned}\tag{1}$$

Here \hat{h}_0 is the fine structure Hamiltonian \hat{H}_{fs} , and the perturbation $\Delta\hat{h}$ is the hyperfine interaction Hamiltonian \hat{H}_{hfs} . In the coupled representation, the eigenstate of \hat{H}_{fs} can be written as

$$|nIJFM_F\rangle = \sum_{M_J, M_I} \langle JM_JIM_I|FM_F\rangle \times |nJM_J\rangle|IM_I\rangle,\tag{2}$$

where n is the principle quantum number, I is the nuclear spin, J is the electronic total angular momentum and $F = I + J$ is the total angular momentum; M_I , M_J and M_F are the projections of I , J and F on the quantization axis, respectively. $\langle JM_JIM_I|FM_F\rangle$ is the Clebsch-Gordan coefficient. However,

*Electronic address: xjzhou@pku.edu.cn

Eq. (2) is not an eigenstate of \hat{h} , because the hyperfine interactions have non-zero off-diagonal matrix elements. In the following, we use a shorthand notation $|i\rangle \equiv |n_i I J F_i M_{F_i}\rangle$ for convenience.

The Green's function of \hat{h} with complex variable z is

$$g_{n_i,i}(z) = \langle i | \frac{1}{z - \hat{h}} | i \rangle = \frac{1}{z - E_{i,fs} - \langle i | \sigma_{i,hfs}^*(z) | i \rangle}, \quad (3)$$

where $\sigma_{i,hfs}^*(z)$ is the proper self-energy, which can be diagrammatically represented by the infinite sum in Fig. (1). Because the hyperfine state energy $E_i = E_{i,fs} + E_{i,hfs}$ is one pole of the Green's function, where $E_{i,fs}$ and $E_{i,hfs}$ are the fine structure energy and the hyperfine corrections, respectively, we have:

$$E_{i,hfs} = \sigma_{i,hfs}^*(E_{i,fs} + E_{i,hfs}) = \sigma_{i,hfs}^*(E_i). \quad (4)$$

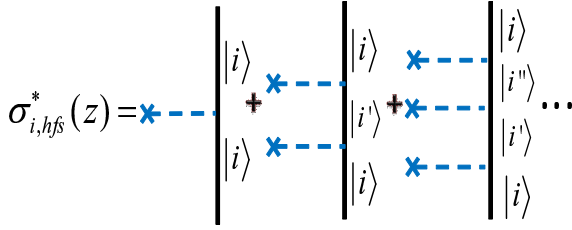


FIG. 1: (Color online) Diagrammatic representation of the proper self-energy $\sigma_{i,hfs}^*(z)$. $|i'\rangle$ and $|i''\rangle$ denote different eigenstates of \hat{H}_{fs} which have the same parity with $|i\rangle$ but with different J or principle quantum numbers. Every solid line(black) marked by $|i\rangle$ represents a factor $g_i^0(z) = 1/(z - \langle i | \hat{H}_{fs} | i \rangle)$. Every dashed line(blue) marked by $|i\rangle$ and $|i'\rangle$ denotes a factor $\langle i | \hat{H}_{hfs} | i' \rangle$. A summation is performed over the index $i', i'' \dots$ in the end.

B. The ac Stark shift

Now we consider a neutral atom in a far-off-resonance laser field with frequency $\nu = \omega/2\pi$. The laser field is assumed to be in a Fock state $|R\rangle = |N\rangle (N \gg 1)$, where N equals the mean photon number. The Hamiltonian \hat{H} of the system can be written as the sum of the unperturbed part \hat{H}_0 and the perturbation $\Delta\hat{H}$:

$$\begin{aligned} \hat{H} &= \hat{H}_0 + \Delta\hat{H}, \\ \hat{H}_0 &= \hat{H}_R + \hat{H}_{fs}, \\ \Delta\hat{H} &= \hat{H}_{hfs} + \hat{H}_e. \end{aligned} \quad (5)$$

Here \hat{H}_0 consists of the radiation field Hamiltonian \hat{H}_R and the fine structure Hamiltonian \hat{H}_{fs} . The state $|i; N\rangle \equiv |i\rangle \otimes |N\rangle$ is an eigenstate of \hat{H}_0 with eigenvalue $E_{i,fs} + N\hbar\omega$.

The perturbation $\Delta\hat{H}$ of Eq.(5) takes into account the hyperfine interaction \hat{H}_{hfs} and atom-photon interaction \hat{H}_e . For \hat{H}_e , we use the dipole approximation $\hat{H}_e = -\hat{d} \cdot \vec{\mathcal{E}}$, where \hat{d} is the electric dipole moment and $\vec{\mathcal{E}}$ is the electric field vector. Here for the sake of simplicity, we have ignored the atom's external degree of freedom.

The Green's function of \hat{H} with complex variable z has a similar form to Eq. (3):

$$G_{i;N}(z) = \langle i; N | \frac{1}{z - \hat{H}} | i; N \rangle = \frac{1}{z - E_{i,fs} - N\hbar\omega - \langle i; N | \Sigma_{i;N}^*(z) | i; N \rangle}, \quad (6)$$

with the proper self-energy

$$\Sigma_{i;N}^*(z) \approx \Sigma_{i;N}^{(0)}(z) + \Sigma_{i;N}^{(2)}(z), \quad (7)$$

where $\Sigma_{i;N}^{(0)}(z)$ and $\Sigma_{i;N}^{(2)}(z)$ are the parts containing the 0th and 2nd order of \hat{H}_e , respectively. Here we have neglected higher orders of atom-photon interactions, due to the reasons presented in the discussion.

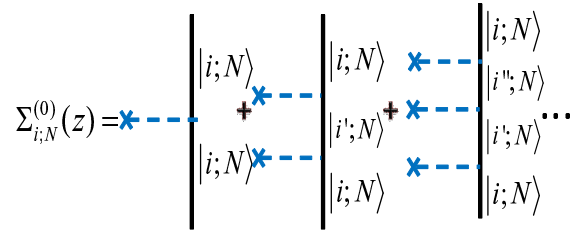


FIG. 2: (Color online) Diagrammatic representation of the proper self-energy $\Sigma_{i;N}^{(0)}(z)$. $|i'\rangle$ and $|i''\rangle$ denote different eigenstates of \hat{H}_{fs} which have the same parity with $|i\rangle$ but with different J or principle quantum numbers. Every solid line(black) marked by $|i; N\rangle$ represents a factor $G_{i;N}^0(z) = 1/(z - \langle i; N | \hat{H}_0 | i; N \rangle)$, and every dashed line(blue) marked by $|i; N\rangle$ and $|i'; N\rangle$ denote a factor $\langle i; N | \hat{H}_{hfs} | i'; N \rangle = \langle i | \hat{H}_{hfs} | i' \rangle$. A summation is performed over the index $i', i'' \dots$ in the end.

The terms in $\Sigma_{i;N}^{(0)}(z)$ and $\Sigma_{i;N}^{(2)}(z)$ can also be represented diagrammatically. In Fig. (2), $\Sigma_{i;N}^{(0)}(z)$ has a similar structure to that of $\sigma_{i,hfs}^*(z)$ except the solid lines represent $G_{i;N}^0(z) = 1/(z - \langle i; N | \hat{H}_0 | i; N \rangle)$, not $g_i^0(z) = 1/(z - \langle i | \hat{H}_{fs} | i \rangle)$. The diagrams of $\Sigma_{i;N}^{(2)}(z)$ are more complicated. It can be decomposed into three kinds of factors: C , D and H , which are presented in Fig. (3):

$$\Sigma_{i;N}^{(2)}(z) = \sum_{\substack{i', i'' \\ j', j''}} C_{i;N}^{i';N} \cdot H_{j'';N\pm 1}^{i'';N} \cdot D_{j';N\pm 1}^{j'';N\pm 1} \cdot H_{i';N}^{j';N\pm 1} \cdot C_{i;N}^{i';N} \quad (8)$$

As shown in the diagram, the hyperfine interactions are included in the C and D factors, meanwhile the H factor contains the atom-photon interactions. The factors C and D are very similar, except in $C_{i;N}^{i';N}$, $|i\rangle$ cannot be an intermediate state, meanwhile in $D_{i;N}^{i';N}$ there is no such restriction. Using

magnetic sublevels $M_{F_1} = M_{F_2} = 0$. The transition frequency shift for the microwave clock is

$$\delta\nu_{clock} = (E_{F_2 M_{F_2}}^{[2+\epsilon]} - E_{F_1 M_{F_1}}^{[2+\epsilon]})/h. \quad (16)$$

A. Numeric results

First, as elaborated in Appendix A, we use the GraspVU program [16] to construct the database of atomic structures of Rb and Cs, including the wavefunctions, energy levels, hyperfine interactions and electric dipole transition strength. With this database, we can calculate the differential ac Stark shift with $E^{[2+\epsilon]}$ method and TOPT. The computation results at various wavelength are presented in Fig.(4) and Fig.(5). We can see both the TOPT values(blue solid line) and $E^{[2+\epsilon]}$ method values(red dashed line) stay negative for all the wavelength and they are very close to each other.

One advantage of $E^{[2+\epsilon]}$ method is that instead of constructing atomic structure data, we can use the existing experimental values of Einstein coefficients and hyperfine energies in Eq.(14). As an illustration, we use experimental values for the hyperfine splittings [17] and transition rates [18, 19]. The calculation results are shown in Fig.(4) and Fig.(5) in black dot-dashed lines. As we can see, they also stay negative for all the wavelength.

Second, we can compare the differential ac Stark shift at specific trapping light wavelength with experimental values. Using TOPT and GraspVU database, the differential shifts at 780 nm and 532 nm with linear polarized light are $-2.00 \times 10^{-2} \text{ Hz/mW/cm}^2$ and $-3.99 \times 10^{-4} \text{ Hz/mW/cm}^2$, while using $E^{[2+\epsilon]}$ method and GraspVU database, the differential shifts are $-1.92 \times 10^{-2} \text{ Hz/mW/cm}^2$ and $-5.59 \times 10^{-4} \text{ Hz/mW/cm}^2$. Both of those results are in agreement with the experimental values $-2.27 \times 10^{-2} \text{ Hz/mW/cm}^2$ and $-3.51 \times 10^{-4} \text{ Hz/mW/cm}^2$ [20]. The $E^{[2+\epsilon]}$ method with experiment database gives $-2.15 \times 10^{-2} \text{ Hz/mW/cm}^2$ and $-6.68 \times 10^{-4} \text{ Hz/mW/cm}^2$, also in agreement with experiments.

B. Order of approximation

In Eq. (12), we have shown that our result is an approximation at the order OC for C factors and OD for D factors. For light shift of ground states of Cesium and Rubidium, OC is the ratio of \hat{H}_{hfs} matrix elements between the ground state and a higher $S_{1/2}$ state to their energy difference, meanwhile OD equals the ratio of \hat{H}_{hfs} matrix elements between two P states to the light detuning. These error terms are very small in typical experiment conditions. Take Rb for example. When $|i\rangle$ is the hyperfine doublet of the ground state, $\Delta E_{i,i'}$ is at least $6 * 10^{14} \text{ Hz}$ meanwhile $\langle i|\hat{H}_{hfs}|i'\rangle$ is at most $2 * 10^9 \text{ Hz}$, which makes $OC \sim O(10^{-5})$. On the other hand, the largest $\langle j|\hat{H}_{hfs}|j'\rangle$ is between $5p$ and $6p$ which is less than $3 * 10^8 \text{ Hz}$, therefore for a wide range of trapping laser wavelength, $OD \sim O(10^{-5})$ can be satisfied. For Cs, a similar estimation can be made. The C factor is approximated at the order $O(3 * 10^9 \text{ Hz}/5 * 10^{14} \text{ Hz}) \sim O(10^{-5})$, and for D factor,

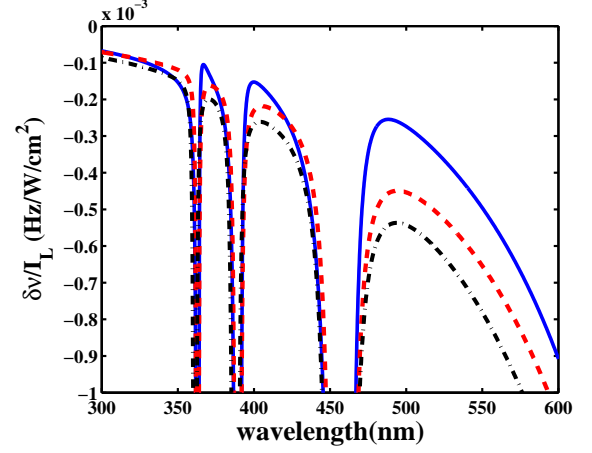


FIG. 4: (Color online) Wavelength dependence of the differential ac Stark shift for the ground state hyperfine doublet of Cesium133. TOPT result using GraspVU data (blue solid), $E^{[2+\epsilon]}$ method result using GraspVU data (red dashed) and $E^{[2+\epsilon]}$ method result using experiment data (black dot-dashed) are presented. The trapping laser wavelength is ranging from 300nm to 600nm.

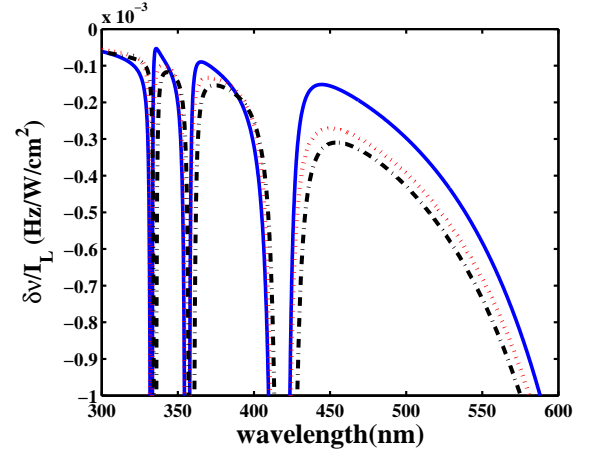


FIG. 5: (Color online) Wavelength dependence of the differential ac Stark shift for the ground state hyperfine doublet of Rubidium87. TOPT result using GraspVU data (blue solid), $E^{[2+\epsilon]}$ method result using GraspVU data (red dashed) and $E^{[2+\epsilon]}$ method result using experiment data (black dot-dashed) are presented. The trapping laser wavelength is ranging from 300nm to 600nm.

the largest $\langle j|\hat{H}_{hfs}|j'\rangle$ is between $6p$ and $7p$ which is about $4 * 10^8 \text{ Hz}$, therefore for a wide range of wavelength of the light field, our method is also valid at the order of accurate $O(10^{-5})$.

However, when we calculate the differential light shift between two hyperfine levels of the ground state, we need to reevaluate the order of accuracy since the light shifts of these two levels are very close to each other. After further investigat-

tion, we discover that for our method to be valid, it requires:

$$\begin{aligned} \max_j \left| \frac{\Delta E_{i,hfs} d_{ij}}{\Delta E_{i,j} - \hbar\omega} \right| &\gg \max_{j,j'} \left| \frac{\langle j | \hat{H}_{hfs} | j' \rangle d_{ij'}}{\Delta E_{i,j'} - \hbar\omega} \right|, \\ \max_j \left| \frac{\Delta E_{i,hfs} d_{ij}^2}{\Delta E_{i,j} - \hbar\omega} \right| &\gg \max_{j',i'} \left| \frac{\langle i | \hat{H}_{hfs} | i' \rangle d_{ij'} d_{i'j'}}{\Delta E_{i,i'}} \right|, \end{aligned} \quad (17)$$

where $|i\rangle$ is the hyperfine level of the ground state, $\Delta E_{i,hfs}$ is the corresponding hyperfine splitting, and $d_{ij} = \langle i | \hat{d} | j \rangle$ is the reduced matrix element of electric dipole operator.

Again take Rb for example. In a far-off-resonant laser field, the first inequality can hold since $\Delta E_{i,hfs} \approx 7 * 10^9 \text{ Hz}$ meanwhile the largest $|\langle j | \hat{H}_{hfs} | j' \rangle| < 4 * 10^8 \text{ Hz}$. In the second inequality, because the largest $|d_{ij}^2/d_{ij'} d_{i'j'}| \geq 5$ and as stated above, $|\langle i | \hat{H}_{hfs} | i' \rangle|/\Delta E_{i,i'} \sim O(2 * 10^9 \text{ Hz}/6 * 10^{14} \text{ Hz})$, it requires the detuning $|\Delta E_{i,j} - \hbar\omega| \ll 10^{16} \text{ Hz}$. A similar analysis can be performed for Cs. This explains why our calculation results of differential light shift are close to the TOPT results, and when the detuning gets bigger, the difference between two results also increases. In conclusion, for a wide range of wavelength of the trapping laser, our method is also valid for calculating the differential light shift of the ground state hyperfine doublet.

IV. DISCUSSIONS AND CONCLUSIONS

In Sec.II, we have derived the $E^{[2+\epsilon]}$ method using the Green's function. In order to obtain the simple expression in Eq.(14) for the ac Stark shift, we have performed a partial summation of the original perturbation expansion of the proper self-energy $\Sigma_{i,N}^*(z)$. The largest contribution to the light shift is the second order process $\Sigma_{i,N}^{*(2)}(z)$. The lowest order diagram $\Sigma_{omit}(z)$ that has been omitted is the fourth order atom-photon interaction, which has an order of magnitude:

$$\Sigma_{omit}(z)/(\Sigma_{i,N}^{*(2)}(z))^2 \approx 1/\Delta, \quad (18)$$

where Δ is the detuning of the radiation field. Take Rb for example. For a wavelength $\lambda = 850 \text{ nm}$ laser field with $20E_R$ trap depth, $\Delta \sim 10^{13} \text{ Hz}$ and $\Sigma_{i,N}^{*(2)}(z) \sim 10^5 \text{ Hz}$, so the ratio $\Sigma_{omit}(z)/\Sigma_{i,N}^{*(2)}(z)$ is much smaller than 10^{-5} and we can keep the atom-photon interaction at the second order.

The calculation results shown in Fig.(4) and Fig.(5) suggest that there is no magic wavelength for Rb and Cs microwave clocks. However, at certain wavelength of trapping laser, the shift difference is very small and varies rather slowly versus the wavelength, implying the differential light shifts would be very stable against the trapping light's intensity and frequency fluctuations. These wavelength are thus suitable for atom trapping in precision measurement. As listed in Table.I, the recommended wavelength obtained using both methods and different databases of atomic structure are very close to each other.

In summary, we have used Green's function to derive the $E^{[2+\epsilon]}$ method Eq. (14) for calculating the ac Stark shift of hyperfine levels. A discussion about the approximation orders

TABLE I: Using TOPT with graspVU data, $E^{[2+\epsilon]}$ with graspVU data and $E^{[2+\epsilon]}$ with experiment data (Expt.), the recommended wavelength λ of trapping laser for Cs and Rb microwave lattice clocks are calculated and listed in the table.

Cs			Rb		
TOPT	$E^{[2+\epsilon]}$	$E^{[2+\epsilon]}$	TOPT	$E^{[2+\epsilon]}$	$E^{[2+\epsilon]}$
(GraspVU)	(GraspVU)	(Expt.)	(GraspVU)	(GraspVU)	(Expt.)
366.8nm	371.2nm	370.4nm	355.8nm	340.0nm	343.0nm
399.8nm	405.2nm	404.0nm	365.2nm	370.2nm	374.0nm
488.2nm	494.2nm	493.8nm	444.4nm	450.0nm	454.2nm
871.2nm	870.2nm	874.8nm	785.4nm	784.8nm	788.2nm

of Eq. (12) is made and we discover that for a wide range of trapping laser wavelength, $E^{[2+\epsilon]}$ method is valid both for calculating the absolute and the differential light shift, which is also indicated by the numerical results. Moreover, the experimental values for atomic levels and Einstein coefficients can be utilized in $E^{[2+\epsilon]}$ method. This implies that $E^{[2+\epsilon]}$ method can be applied to other group elements for which *ab initio* atomic structure databases are difficult to construct.

ACKNOWLEDGMENTS

We thank Thibault Vogt for having carefully reviewed our article. This work is partially supported by the state Key Development Program for Basic Research of China (No.2011CB921501) and NSFC (No.11334001), RFDP (No.20120001110091).

Appendix A: Numerical calculation of atom structure data

We use the GraspVU code [16] which is based on the relativistic multi-configuration Dirac-Fock (MCDf) method [21] to compute the energy levels and generate the wave functions. In the following, we first present a brief summary of the MCDf method and our calculation strategies. For an N -electron atom or ion, the Dirac-Coulomb Hamiltonian can be expressed as (in atomic unit)

$$\hat{H}_{DC} = \sum_{i=1}^N [c\alpha p_i + (\beta - 1)c^2 - \frac{Z}{r_i}] + \sum_{i=1}^{N-1} \sum_{j=i+1}^N |r_i - r_j|^{-1}. \quad (A1)$$

So the eigenvalue problem is

$$\hat{H}_{DC} |\Gamma P J M\rangle = E_\Gamma |\Gamma P J M\rangle. \quad (A2)$$

Where $|\Gamma P J M\rangle$ represents the atomic state functions (ASFs) with Γ denoting other quantum numbers. The ASF can be written as linear combinations of configuration state functions

(CSFs) with the same parity P , total angular momentum J and magnetic quantum number M ,

$$|\Gamma P J M\rangle = \sum_{i=1}^{n_c} C_i^\Gamma |\gamma_i P J M\rangle. \quad (\text{A3})$$

Here C_i^Γ is the mixing coefficients, γ_i represents all information required to define CSF uniquely, and n_c is the number of CSFs. The CSFs $|\gamma_i P J M\rangle$ which form a quasi-complete basis set in Hilbert space are linear combinations of Slater determinants of order N constructed from atomic orbital functions (AOs). By applying variational method to Eq.(B2), we can obtain the mixing coefficients and the AOs self-consistently. Our calculations are based on our recently

TABLE II: Calculation strategies of the atomic orbital sets for Cs and Rb.

	step 1 ^a	step 2	step 3	step 4	step 5	step 6 ^b	step 7
Cs	1*,2*,3*,4s 4p,4d,5s,5p	6s,6p 5d	7s,7p 6d	8s,4f 8p,7d	9s,5f 9p,8d	$\overline{10s,10p}$ $\overline{9d,6f}$	$\overline{11s,11p}$ $\overline{10d,7f}$
Rb	1*,2*,3* 4s,4p	5s,5p 4d	6s,6p 5d	7s,7p 6d	8s,4f 8p,7d	$\overline{9s,9p}$ $\overline{8d,5f}$	$\overline{10s,10p}$ $\overline{9d,6f}$

^a 1* represents 1s spectroscopy orbital, 2* represents 2s,2p spectroscopy orbitals while 3* represents 3s,3p and 3d spectroscopy orbitals

^b \overline{nl} represents pseudo orbital

proposed multi-configuration self-consistent field (MCSCF) strategies [22, 23]. We use GraspVU code [16] to optimize a set of high-quality orbital basis where pseudo orbitals [13, 22–25] are included, by which we can take into account the electron correlation effects adequately. The pseudo orbitals determined by variational method are specific linear combinations of infinite bound type orbitals and continuum orbitals. More specifically, the occupied orbitals are obtained from ground

state single configuration calculations. The other AOs are obtained through MCSCF calculations with all the core orbitals fixed. For Cs, we first extend the AOs classified by manifold v of effective quantum numbers to 9s, 9p, 8d, 5f by optimizing the orbitals with same angular momentum l separately. These orbitals are treated as spectroscopy orbitals (labeled as nl and with fixed number of radial nodes, i.e. $n - l - 1$), and they represent the physical state. Configurations are generated by single excitation from 6s¹ and all the energy levels are optimized. Note that these spectroscopy orbitals are adequate for polarizability calculations in present frequency scale. In order to consider electron correlations adequately, we further extend the AOs as pseudo orbitals (labeled as \overline{nl} and without restriction on radial nodes) to $\overline{11s}$, $\overline{11p}$, $\overline{10d}$, $\overline{7f}$ by optimizing the orbitals with same angular momentum l separately. With all the spectroscopy orbitals included, the configurations are generated by single and double excitations only allowing one electron excited from 5p or 6s orbitals. The optimized energy levels are the same as in the spectroscopy orbital calculations. We call the basis set which satisfies the desired accuracy of calculations quasi-complete basis set, as listed in Table.II. The quasi-complete basis set for Rb is constructed in the same way as Cs.

All the calculations in this work depend on the quasi-complete basis obtained in the previous procedure. To verify the quality of this basis, we first perform configuration interaction calculations (CI) with configuration generated by single and double excitations from 5p⁶6s¹. With Breit interactions included, the fine-structure energy levels of ns , np ($5 \leq n \leq 9$ for Cs, $4 \leq n \leq 8$ for Rb) states agree with the experimental results within 1%, both for Cs and Rb. Hence, the correlations are considered adequately and the ASFs should be adequate for further calculation. By using these ASFs, the transition parameters and transition matrix elements for electric dipole transitions are calculated, and the hyperfine interaction such as the magnetic dipole interaction (A constants) and electric quadrupole interaction (B constants) are computed. The off-diagonal hyperfine interaction elements on the $|F, M_F\rangle$ basis in Eq. (2) can also be obtained from RHFS [26].

-
- [1] A. A. Madej, P. Dub, Z. Zhou, J. E. Bernard, and M. Gertssof, Phys. Rev. Lett. **109**, 203002 (2012).
 - [2] T. Rosenband et al., Science **319**, 1808 (2008).
 - [3] P. Bakopoulos, D. Tsiokos, O. Zouraraki, H. Avramopoulos, G. Maxwell, and A. Poustie, Opt. Express **13**, 6401 (2005)
 - [4] R. Grimm, M. Weidemuller, and Y. B. Ovchinnikov, Optical Dipole Traps for Neutral Atoms, Adv. Atom. Mol. Opt. Phys. **42**, 95 (2000).
 - [5] H. Katori, M. Takamoto, V. G. Pal'chikov, and V. D. Ovsiannikov, Phys. Rev. Lett. **91**, 173005 (2003).
 - [6] G. K. Campbell, A. D. Ludlow, S. Blatt, J. W. Thomsen, M. J. Martin, M. H. G. de Miranda, T. Zelevinsky, M. M. Boyd, J. Ye, S. A. Diddams, T. P. Heavner, T. E. Parker, and S. R. Jefferts, Metrologia **45**, 539 (2008).
 - [7] S. Blatt, A. D. Ludlow, G. K. Campbell, J. W. Thomsen, T. Zelevinsky, M. M. Boyd, and J. Ye, Phys. Rev. Lett. **100**, 140801 (2008).
 - [8] A. D. Ludlow, T. Zelevinsky, G. K. Campbell, S. Blatt, M. M. Boyd, M. H. G. de Miranda, M. J. Martin, J. W. Thomsen, S. M. Foreman, J. Ye, T. M. Fortier, J. E. Stalnaker, S. A. Diddams, Y. Le Coq, Z. W. Barber, N. Poli, N. D. Lemke, K. M. Beck, and C. W. Oates, Science **319**, 1805-1808 (2008).
 - [9] X. J. Zhou, X. Z. Chen, J. B. Chen, Y. Q. Wang and J. M. Li, Chin. Phys. Lett. **26**, 090601 (2009).
 - [10] G. Wilpers, C. Oates, and L. Hollberg, Applied Physics B: Lasers and Optics **85**, 31 (2006).
 - [11] Z. W. Barber, C. W. Hoyt, C. W. Oates, L. Hollberg, A. V. Taichenachev, and V. I. Yudin, Phys. Rev. Lett. **96**, 083002 (2006).
 - [12] Z. W. Barber, J. E. Stalnaker, N. D. Lemke, N. Poli, C. W.

- Oates, T. M. Fortier, S. A. Diddams, L. Hollberg, C. W. Hoyt, A. V. Taichenachev and V. I. Yudin, Phys. Rev. Lett. **100**, 103002 (2008).
- [13] X. Gao and J. M. Li, Chin. Phys. Lett. **27**, 063101 (2010).
- [14] X. J. Zhou, X. Xu, X. Z. Chen and J. B. Chen, Phys. Rev. A **81**, 012115 (2010).
- [15] A. Derevianko and H. Katori, Rev. Mod. Phys. **83**, 331 (2011).
- [16] F. A. Parpia, C. F. Fischer, and I. P. Grant, Comput. Phys. Com. **94**, 249 (1996).
- [17] E. Arimondo, M. Inguscio and P. Violino, Rev. Mod. Phys. **49**, 31 (1977).
- [18] NIST Atomic Spectra Database, http://physics.nist.gov/cgi-bin/AtData/main_asd.
- [19] R. J. Rafac, C. E. Tanner, A. E. Livingston, and H. G. Berry, Phys. Rev. A **60**, 3648 (1999).
- [20] P. Rosenbusch, S. Ghezali, V. A. Dzuba, V. V. Flambaum, K. Beloy and A. Derevianko, Phys. Rev. A **79**, 013404 (2009).
- [21] I. P. Grant, Adv. Phys. **19**, 747 (1970).
- [22] B. Qing, C. Cheng, X. Gao, X. L. Zhang and J. M. Li, Acta. Phys. Sin. **59**, 145 (2010).
- [23] S. H. Chen, B. Qing and J. M. Li, Phys. Rev. A **76**, 042507 (2007).
- [24] C. Cheng, X. L. Zhang, X. Gao, B. Qing and J. M. Li, J. Phys. B: At. Mol. Opt. Phys. **43**, 105001(2010).
- [25] X. L. Zhang, C. Cheng, X. Gao and J. M. Li, Chin. Phys. Lett. **27**, 033101 (2010).
- [26] P. Jönsson, F.A. Parpia, C. F. Fischer, Comput. Phys. Com. **96**, 301 (1996).